Segmentation of Blood Vessels and Optic Disc In

Kota Prajwal Kant,

Gandhi institute of advanced computer and research Dept of ECE,

Abstract:- Retinal image analysis is increasingly prominent as a non-intrusive diagnosis method in modern ophthalmology. In this paper, we present a novel method to segment blood vessels and optic disc in the fundus retinal images. The method could be used to support non-intrusive diagnosis in modern ophthalmology since the morphology of the blood vessel and the optic disc is an important indicator for diseases like diabetic retinopathy, glaucoma and hypertension. Our method takes as first step the extraction of the retina vascular tree using the graph cut technique. The blood vessel information is then used to estimate the location of the optic disc. The optic disc segmentation is performed using two alternative methods. The Markov Random Field (MRF) image reconstruction method segments the optic disc by removing vessels from the optic disc region and the Compensation Factor method segments the optic disc using prior local intensity knowledge of the vessels. The proposed method is tested on three public data sets, DIARETDB1, DRIVE and STARE. The results and comparison with alternative methods show that our method achieved exceptional performance in segmenting the blood vessel and optic disc.

Index Terms:- Retinal images, vessel segmentation, optic disc segmentation, graph cut segmentation.

I.   INTRODUCTION

The segmentation of retinal image structure has been of great interest because it could as a non intrusive diagnosis in modern ophthalmology. The morphology of the retinal blood vessel and the optic disc is an important structural indicator for assessing the presence and severity of retinal diseases such as diabetic retinopathy, hypertension, glaucoma, haemorrhages, vein occlusion and neo-vascularisation. However to assess the diameter and tortuosity of retinal blood vessel or the shape of the optic disc, manual planimetry has commonly been used by ophthalmologist, which is generally time consuming and prone with human error, especially when the vessel structure are complicated or a large number of image are acquired and prone with human error , especially when the vessel structure are compited or a large number of images are acquired to be labeled by hand . therefore a reliable automated methos for retinal blood vessel and optic disc segmentation, which preserves various vessel and optic disc characteristics is attractive in computer aided-diagnosis. An automated segmentation and inspection of retinal blood vessel features such as diameter, colour and tortuosity as well as the optic disc morphology allows ophthalmologist and eye care specialists to perform mass vision screening exams for early detection of retinal diseases and treatment evaluation. This could prevent and reduce vision impairments; age related diseases and many cardiovascular diseases as well as reducing the cost of the screening.

Over the past few years, several segmentation techniques have been employed for the segmentation of retinal structures such as blood vessels and optic disc and diseases like lesions in fundus retinal images. However the acquisition of fundus retinal images under different conditions of illumination, resolution and field of view (FOV) and the overlapping in the retina cause a significant to the performance of automated blood vessel and optic disc segmentations. Thus, there is a need for a reliable technique for retinal vascular tree extraction and optic disc detection, which preserves various vessel and optic disc shapes. In the following segment, we briefly review the previous studies on blood vessel segmentation and optic disc segmentation separately.

II.   RELATED WORKS

Two different approaches have been developed to segment the vessels of the retina. The pixel processing based method and tracking method The pixel processing based approach performs the vessel segmentation in a two-pass operation. First the appearance of the vessel is enhanced using detection process such as morphological pre processing techniques and adaptive filtering. The second operation is the recognition of vessel structure Using thinning or branch point operation to classify a pixel as a vessel background. These approaches process every pixel in the image apply multiple operation on each pixel.   The second set of approaches to vessel segmentation are referred to as vessel tracking, vectorial tracking or tracing [1]. In contrast

to the pixel processing based approaches, the tracking methods detect first initial vessel seed points, and then track the rest of the vessel pixels through the image by measuring the continuity proprieties of the blood vessels. This technique is used as a single pass operation, where the detection of the vessel structures and the recognition of the structures are simultaneously performed.

The tracking based approaches included semi automated tracing and automated tracing. In the semi automated tracing methods, the user manually selects the initial vessel seed point. These methods are generally used in quantitative coronary angiography analysis and they generally provide accurate segmentation of the vessels. In fully automated tracing, the algorithms automatically select the initial vessel points and most methods use Gaussian functions to characterise a vessel profile model, which locates a vessel points for the vessel tracing. They are computationally efficient and more suitable for retinal image processing. Examples of the tracking based approaches are presented in Xu et al. [8], Maritiner-perez et al. [9], Staal et al. [5], Zhou et al [10].

Both pixel processing and tracking approaches have their own advantages and limitations over each other. The pixel processing approaches can provide a complete extraction of the vascular tree in the retinal image since they search all the possible vessel pixels across the whole image. However these techniques are computationally expensive and require special hardware to be suitable for large image dataset. The presence of noise and lesions in some retinal images causes a significant degradation in the performance of the pixel processing approaches as the enhancement operation may pick up some noise and lesions as vessel pixels. This could lead to false vessel detection in the recognition operation. On the other hand, the tracking approaches are computationally efficient and much faster than the pixels processing methods because they perform the vessel segmentation using only the pixels in the neighbourhood of the vessels structure and avoid the processing of every pixel in the image. Nevertheless, these methods lack in extracting a complete vascular tree in the case where there are discontinuities in the vessel branches. Further more, the semi automated tracking segmentation methods need manual input, which requires time.

The optic nerve head is described as the brightest round area in the retina where the blood vessels converge with a shape that is approximately elliptical and has a width of 1.8 ± 0.2 mm and height 1.9 ± 0.2 mm [11]. The convergence feature of blood vessels into the optic disc region is generally used to estimate the location of the optic disc and segment it from the retinal image. But the intrusion of vessels in the optic disc region constitutes computational complexity for the optic disc segmentation as it is breaking the continuity of its boundary. To address this problem, several methods have been employed such as Chrastek et al. [12], Lowell et al. [13], Welfer et al. [14] and Aquino et al. [15] . Chrastek et al. [12] presented an automated segmentation of the optic nerve head for diagnosis of glaucoma. The method removes the blood vessel by using a distance map.

algorithm, then the optic disc is segmented by combining a morphological operation, Hough Transform and an anchored active contour model. Lowell et al. [13] proposed a deformable contour model to segment the optic nerve head boundary in low resolution retinal images. The approach localises the optic disc using a specialised template matching and a directionally-sensitive gradient to eliminate the obstruction of the vessel in the optic disc region before performing the segmentation. Welfer et al. [14] proposed an automated segmentation of the optic disc in colour eye fundus image using an adaptive morphological operation. The method uses a watershed transform markers to define the optic disc boundary and the vessel obstruction is minimised by morphological erosion.

These techniques are performed using morphological operations to eliminate the blood vessels from the retinal image. However, the application of morphological operations can modify the image by corrupting some useful information.

In our optic disc segmentation process, the convergence feature of vessels into the optic disc region is used to estimate its location. We then use two automated methods (Markov Random field image reconstruction and Compensation Factor) to segment the optic disc.

The rest of the paper is organised as follow. The blood vessel segmentation is discussed in Section III. Section IV provides the detailed description of the optic disc segmenta- tion. Section V presents the experimental results of our method with comparisons to other methods. Conclusions are drawn in Section VI. The preliminary results of the three components of the approach, namely the blood vessel segmentation, optic disc segmentation using the Graph Cut and Markov Random Field respectively, were presented separately in [16], [17], [18]. More details of the approach can be found in the PhD thesis [19].

III. BLOOD VESSELS SEGMENTATION

Blood vessels can be seen as thin elongated structures in the retina, with variation in width and length. In order to segment the blood vessel from the fundus retinal image, we have implemented a pre-processing technique, which consists of effective adaptive histogram equalisation (AHE) and robust distance transform. This operation improves the robustness and the accuracy of the graph cut algorithm. Fig. 1 shows the illustration of the vessel segmentation algorithm.
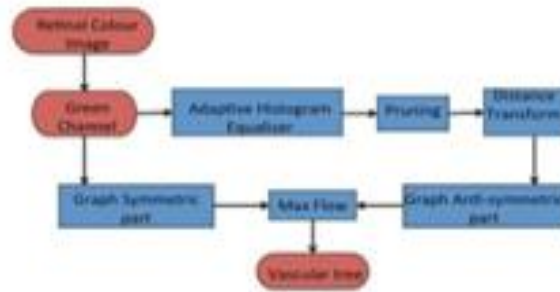

Fig. 1. Vessel segmentation algorithm

A. Pre-processing

We apply a contrast enhancement process to the green channel image similar to the work presented in [20]. The intensity of the image is inverted, and the illumination is equalised. The resulting image is enhanced using an adaptive histogram equaliser, given by:

EQ1

where I is the green channel of the fundus retinal colour image, p denotes a pixel and p^0 is the neighbourhood pixel around p. p^0 2 R(p) is the square window neighbourhood with length h. s(d) = 1 if d > 0, and s(d) = 0 otherwise with d = s (I (p) I (p^0)). M = 255 value of the maximum intensity in the image. r is a parameter to control the level of enhancement. Increasing the value of r would also increase the contrast between vessel pixels and the background (see Fig. 2). The experimental values of the window length was set to h = 81 and r = 6.

A binary morphological open process is applied to prune the enhanced image, which discards all the misclassified pixels see (Fig. 2 (d)). This approach significantly reduces the false positive, since the enhanced image will be used to construct the graph for segmentation.

A distance map image is created using the distance transform algorithm. This is used to calculate the direction and magnitude of the vessel gradient. Fig. 2 (e) and (f) show the distance map of the whole image and a sample vessel with arrows indicating the direction of the gradients respectively. From the sample vessel image, we can see the centre line with the brightest pixels, which are progressively reduced in intensity in the direction of the edges (image gradients). The arrows in Fig. 2 (f) referred as vector field, which is used to construct the graph in the next Sections.

IV. GRAPH CONSTRUCTION FOR VESSEL SEGMENTATION

The graph cut is an energy based object segmentation approach. The technique is characterised by an optimisation
operation designed to minimise the energy generated from a given image data. This energy defines the relationship between neighbourhood pixel elements in an image.
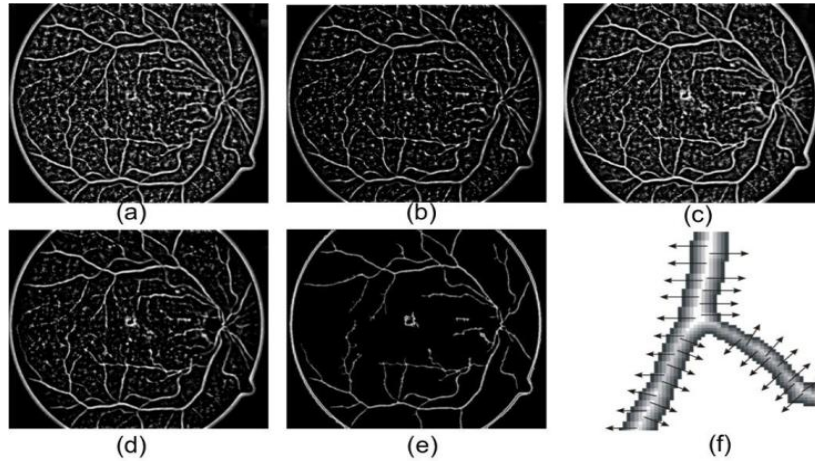
A graph G (;) is defined as a set of nodes (pixels) and a set of undirected edges that connect these neighbouring nodes. The graph included two special nodes, a foreground terminal (source S) and a background terminal (sink T). includes two types of undirected edges: neighbourhood links (n-links) and terminal links (t-links). Each pixel p 2 P (a set of pixels) in the graph presents two t-links fp; Sg and fp; T g connecting it to each terminal while a pair of neighbouring pixels fp; qg 2 N (number of pixel neighbour) is connect by a n-links [21]. Thus:

EQ 2
An edge e 2 is assigned a weight (cost) $W_e > 0$. A cut is defined by a subset of edges C 2 where G (c) = h ; nCi separating the graph into two foreground and background with

EQ 3
The graph cut technique is used in our segmentation because it allows the incorporation of prior knowledge into the graph formulation in order to guide the model and find the optimal segmentation. Let assume A = (A_1; A_p; : : : A_P) a binary vector set of labels assigned to each pixel p in the image, where A_p indicate assignments to pixels p in P . Therefore, each assignment A_p is either in foreground (F g) or background (Bg). Thus the segmentation is obtained by the binary vector A and the constraints imposed on the regional and boundary proprieties of vector A are derived by the energy formulation of the graph defined as

EQ 4
where the positive coefficient λ indicates the relative impor- tance of the regional term (likelihoods of foreground and back- ground) *RA* against the boundary term (relationship between neighbourhood pixels) *BA*. The regional or the likelihood of the foreground and background is given by
EQ 5 6 7
During the minimisation of the graph energy formulation in
to segment thin objects like blood vessels, the second term (boundary term) in (4) has a tendency to follow short edges known as "the shrinking bias" [22]. This problem causes a significant degradation on the performance of the graph cut algorithm on thin elongated structures like the blood vessels. Fig. 3 shows an example of the blood vessel segmentation using the traditional graph formulation [23]. From Fig. 3, it can be seen that the blood vessel segmentation follows short edges, and tends to shrink in the searching for the cheapest cost. It can also be noticed that λ in (4) controls the relation between boundary and regional terms. Increasing the value of λ, the likelihood of the pixels belonging to foreground and
background (t-links) gains strength over the regional term (n-links), which slightly improved the segmentation result see

Fig. 3 (d).
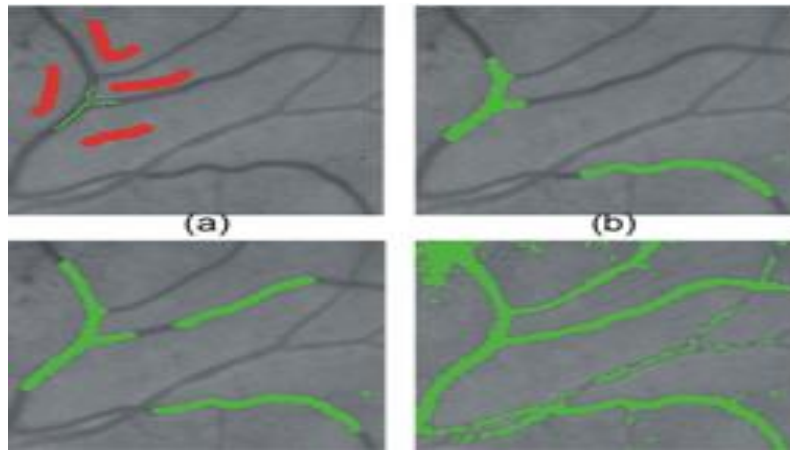
To address the above problem, the segmentation of blood vessels using the graph cut requires special graph formulation. One of the method used to address the shrinking bias problem
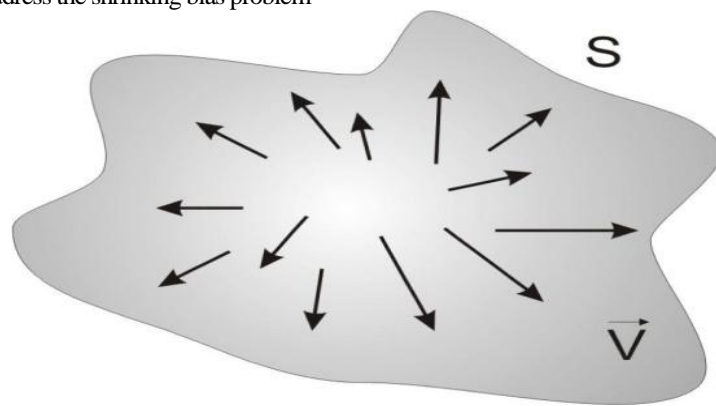
described geometric proprieties of the discrete cut metric on regular grids and Finsler length can be represented by the sum of two terms. Those terms represent the symmetric and anti-symmetric parts of the cut metric. The symmetric part of the cut defines the standard geometric length of contour and it is independent of its orientation. The anti-symmetric part of the cut metric represents the flux of a given vector field through the contour [23].

To address "the shrinking bias" problem seen in Fig. 3, we have constructed a graph consisting of a symmetric part $g+$ (shrinking) and an anti-symmetric part $g-$ (stretching) by incorporating the flux of vector v into the graph construction. The symmetric part $g+$ of the graph corresponds to a cut geometric length and is related directly with the n-link connections and the anti-symmetric part $g-$ is equal to flux of vector field v over the cut geometric and it is used to derive the t-links. Thus the the blood vessels can be segment by keeping a good balance between shrinking and stretching (flux) throughout the image boundary.

1)   *The symmetric part of the graph:* is used to assign weights on the n-link connections (edges
2)   between neigh- bouring pixels). Let consider a neighbour system of a graph described by a set of edges ek , where $1 \leq k \leq N$, for N number of neighbours. Let us define ek as the shortest vector

connecting two pixels in the direction of k, $W^+(p)$ the weight
of the edge ek at pixel p and $W(p)$ a set of the edge weights at pixel p for all directions. The corresponding edge weights are defined by

The anti-symmetric part of the graph : We used the term Anti-Symmetry because, the flux (stretching) of vector field v over the cut geometric balanced the shrinking of blood vessels during the segmentation. This anti-symmetric part of the graph is defined by the flux of vector field v over the cut geometric. It is used to assign weights on the t-links (edges between a given pixel and the terminals) to balance the shrinking effect seen in Fig. 3. Specific weights for t-links are obtained based on the deposition of vector v. Different decompositions of vectorv may result in different t-links whose weights can be interpreted as an estimation of divergence. In our

implementation, we decomposed the vector v along grid edges with the n-links oriented along the main axes, X and Y direction. Thus vector v can be decomposed as $v = v_x u_x + v_y u_y$ where u_x and u_y are unit vectors in X

EQ 10

where v_x^{right} and v_x^{right} are the components of vector v in X direction taken at the right and left neighbour of pixel P respectively. v_y^{up} and v_y^{down} are the Y of vector v taken at the top and down of of pixel P . is the size of the cell in the grid map (see Fig. 5). We add edge (s ! p) with weight C (tp) if tp < 0, or edge (p ! t) with weight C tp otherwise. The parameter C is related to the magnitude of the vector v, thus pixels in the centre of the blood vessel have a higher connection to the source (foreground) than pixels in the edge of the blood vessels. Because the distance map is calculated on the pruned image and vector v is only defined for the pixels detected as blood vessels in the

rough segmentation. For the rest of the pixels in the image, the initialisation of t-link weights is set as (p ! s) with weight t = 0 and (p ! t) with weight t = K, where K is the maximum weight sum for a pixel in the symmetric construction. Fig. 6 shows the segmentation results of the blood vessels using different decomposition of the vector v generating different t-link weights
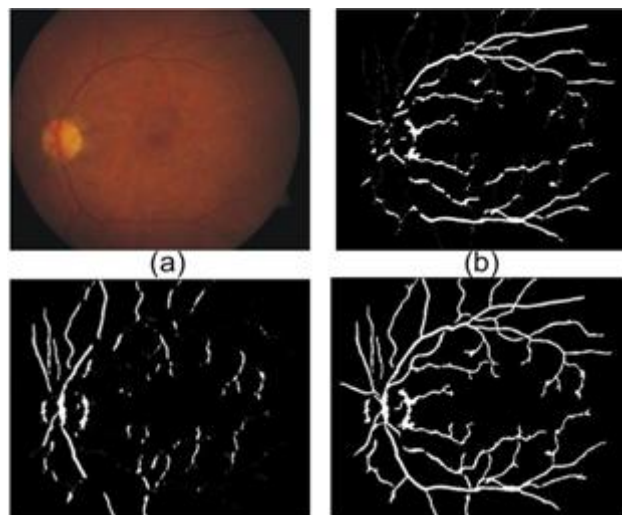
V.   OPTIC DISC SEGMENTATION

The optic disc segmentation starts by defining the location of the optic disc. This process used the convergence feature of vessels into the optic disc to estimate its location. The disc area is then segmented using two different automated methods (Markov Random field image reconstruction and Compensation Factor). Both methods use the convergence feature of the vessels to identify the position of the disc. The Markov Random Field (MRF) method is applied to eliminate the vessel from the optic disc region. This process is known as image reconstruction and it is performed only on the vessel pixels to avoid the modification of other structures of the image. The reconstructed image is free of vessel and it is used to segment the optic disc via graph cut. In contrast to MRF method, the Compensation Factor approach segments the optic disc using prior local intensity knowledge of the vessels. Fig. 7 shows the overview of both the MRF and the Compensation Factor method process.
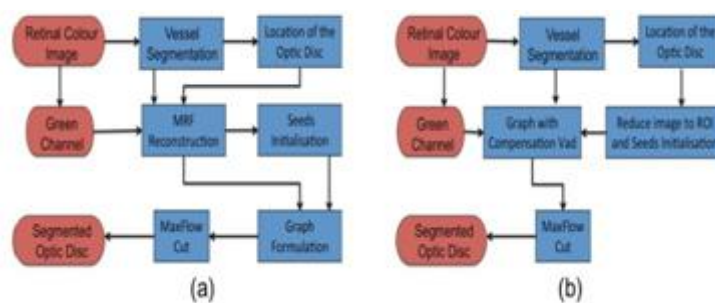

FIG6

image of vessels segmented in Section III to find the location of the optic disc. The process iteratively trace towards the centroid of the optic disc. The vessel image is pruned using a morphological open process to eliminate thin vessels and keep the main arcade. The centroid of the arcade is calculated using the following formulation:

$$C_x = \frac{\sum_{i=1}^{K} x_i}{K} \qquad C_y = \frac{\sum_{=1}^{K} y_i}{K} \qquad (12)$$

where x_i and y_i are the coordinates of the pixel in the binary image and K is the number of pixels set to 1 (pixels marked as blood vessels) in the binary image.

Given the gray scale intensity of a retinal image, we select 1% of the brightest region. The algorithm detects the brightest region with the most number of pixels to determine the location of the optic disc with respect to the centroid point (right, left, up or down). The algorithm adjusts the centroid point iteratively until it reaches the vessel convergence point or centre of the main arcade (centre of the optic disc) by reducing the distance from one centroid point to next one in the direction of the brightest region, and correcting the central position inside the arcade accordingly. Fig. 8 shows the process of estimating the location of the of optic disc in a retinal image. It is important to notice that, the vessel convergence point must be detected accurately, since this point is used to automatically mark foreground seeds. A point on the border of the optic disc may result in some false foreground seeds. After the detection of the vessel convergence point, the image is constrained a region of interest (ROI) including the whole area of the optic disc to minimize the processing time. This ROI is set to a square of 200 by 200 pixels concentric with the detected optic disc centre. Then an automatic initialisation of seeds (foreground and background) for the graph is performed. A neighbourhood of 20 pixels of radius around the centre of the optic disc area is marked as foreground pixels and a band of pixels around the perimeter of the image are selected as background seeds (see Fig. 9).

B. Optic Disc Segmentation with Markov Random Field Image Reconstruction

The high contrast of blood vessels inside the optic disc presented the main difficulty for it segmentation as it misguides the segmentation through a short path, breaking the continuity of the optic disc boundary. To address this problem, the MRF based reconstruction method presented in [25] is adapted in our work. We have selected this approach because of its robustness. The objective of our algorithm is to find a best match for some missing pixels in the image, however one of the weaknesses of MRF based reconstruction is the requirement of intensive computation. To overcome this problem, we have limited the reconstruction to the region of interest (ROI) and using prior segmented retina vascular tree, the reconstruction was performed in the ROI. An overview diagram of the optic disc segmentation with Markov Random Field Image Reconstruction is shown in Fig. 6.

FIG 7,8

Let us consider a pixel neighbourhood $w(p)$ define as a square window of size W, where pixel p is the centre of the neighbourhood . I is the image to be reconstructed and some of the pixels in I are missing. Our objective is to find the best approximate values for the missing pixels in I. So let $d(w1; w2)$ represent a perceptual distance between two patches that defines their similarity. The exact matching patch corresponds to $d(w^0; w(p)) = 0$. If we define a set of these patches as $(p) = f!^0 \ I : d(!^0; !(p)) = 0g$ the probability density function of p can be estimated with a histogram of all centre pixel values in (p). However we are considering a finite neighbourhood for p and the searching is limited to the image area, there might not be any exact matches for a patch. For this reason, we find a collection of patches, which match falls between the best match and a threshold. The closest match is calculated as $!_{best} = \text{argmin}_! d(!(p); !) \ I$. All the patches ! with $d(!(p); !) < (1 +)d(!(p); !_{best})$ are included in the collection $!^0$. $d(w^0; w(p))$ is defined as the sum of the absolute differences of the intensities between patches, so identical patches will result in $d(w^0; w(p)) = 0$. Using the collection of patches, we create an histogram and select the one with the highest mode. Fig. 10 shows sample results of the reconstruction. The foreground $F \ g_s$ and the background

The graph cut algorithm described in section III-B is used to separate the foreground and the background by minimising the energy function over the graph and producing the optimal segmentation of the optic disc in the image. The energy function of the graph in (4) consists of regional and boundary terms. The regional term (likelihoods of foreground and background) is calculated using (5), while the boundary term

(relationship between neighbouring pixels) is derived using (6). A grid of 16 neighbours N is selected to create links between pixels in the image Im. The Max-Flow algorithm is used to cut the graph and find the optimal segmentation.

C. Optic Disc Segmentation With Compensation Factor

In contrast to MRF image reconstruction, we have incorporated the blood vessels into the graph cut formulation by introducing a compensation factor V ad. This factor is derived using prior information of blood vessel.

The energy function of the graph cut algorithm generally comprises a boundary and regional terms. The boundary term defined in (6) is used to assign weights on the edges (n-links) to measure the similarity between neighbouring pixels with respect to the pixel proprieties (intensity, texture, colour). Therefore pixels with similar intensities have a strong connec-tion. The regional term in (5) is derived to define the likelihood of the pixel belonging to the background or the foreground by assigning weights on the edges (t-link) between image pixels and the two terminals background and foreground seeds. In order to incorporated the blood vessels into the graph cut formulation, we derived the t-link as follows:

$$S_{link} = \begin{array}{l} \ln P_r \ (I_p nF \ g_{seeds}) + V \ ad \ if \ p = vessel \\ \ln P_r \ (I_p nF \ g_{seeds}) \ if \ p \ 6= vessel \end{array}$$

The intensity distribution of the blood vessel pixels in the region around the optic disc makes them more likely to belong to background pixels than the foreground (or the optic disc pixels). Therefore the vessels inside the disc have weak connections with neighbouring pixels making them likely to be segmented by the graph cut as background. We introduce in (13) a compensation vector to all t-links of the foreground for pixels belong to the vascular tree to address this behaviour. Consequently, vessels inside the optic disc are classified with respect to their neighbourhood connections instead of their likelihood with the terminals foreground and background seeds. Fig. 11 shows sample of images segmented by Compensation Factor. The segmentation of the disc is affected by the value of *V ad*, the method achieves poor segmentation results for low value of *V ad*. However when the value of the *V ad* increases, the performance improves until the value of *V ad* is high enough to segment the rest of the vessels as foreground.

VI.   RESULTS

For the vessel segmentation method, we tested our algorithm on two public datasets, DRIVE [5], STARE [2] with a total of 60 images. The optic disc segmentation algorithm was tested on DRIVE [5] and DIARETDB1 [26], consisting of 129 images in total. The performance of both methods is tested against a number of alternative methods.

The DRIVE consists of 40 digital images which were captured from a Canon CR5 non-mydriatic 3CCD camera at 45◦ field of view (FOV). The images have a size of 768 × 584

whereas the set B provides the manually labelled images for half of the dataset. To test our method we adopt the set A hand labelling as the benchmark. We manually delimited the optic disc to test the performance of optic disc segmentation algorithm.

The STARE dataset consists of 20 images captured by a TopCon TRV-50 fundus camera at 35◦ FOV. The size of the images is 700 × 605 pixels. We calculated the mask image for this dataset using a simple threshold technique for each

colour channel. The STARE dataset included images with retinal diseases selected by Hoover et al [2]. It also provides two sets of hand labelled images performed by two human experts. The first expert labelled fewer vessel pixels than the second one. To test our method we adopt the first expert hand labelling as the ground truth.

The DIARETDB1 dataset consist of 89 colour images with 84 of them contain at last one indication of lesion. The images were captured with digital fundus camera at 50 degree filed of view and have a size of 1500 × 1152 pixels. Hand labelled lesion regions are provided in this dataset by four human experts. However the DIARETDB1 dataset only

includes the hand labelled ground truth of lesions but not the blood vessels and the optic disc. For this reason, we were unable to compare the performance of the blood vessel segmentation on the DIARETDB1 dataset. Nevertheless we were able to create the hand labelled ground truth of optic disc to test the performance of the optic disc segmentation.

To facilitate the performance comparison between our method and alternative retinal blood vessels segmentation approaches, parameters such as the true positive rate (TPR), the false positive rate (FPR) and the accuracy rate (ACC) are derived to measure the performance of the segmentation [5]. The accuracy rate is defined as the sum of the true positives (pixels correctly classified as vessel points) and the true negatives (non-vessel pixels correctly identified as non vessel points), divided by the total number of pixel in the images. True Positive Rate (TPR) is defined as the total number of true positives, divided by the number of blood vessel pixel marked in the ground true image. False Positive Rate (FPR) is calculated as the total number of false positives divided by the number of pixels marked as non-vessel in the ground true image. It is worth mentioning that a perfect segmentation would have a FPR of 0 and a TPR of 1. Our method and all the alternative methods used the first expert hand labelled images as performance reference.

Most of the alternative methods use the whole image to measure the performance. In [5] all the experiments are done on the FOV without considering the performance in the dark area outside the FOV. The method in [3] measures the performance on both the whole image and the FOV. The

For the optic disc segmentation Tables V and VI present the performance of our method on DIARETDB1 and DRIVE images. The results show that our methods of using (the Compensation factor and the MRF image reconstruction) achieved the best overall performance. The results also show that, the MRF image reconstruction algorithm outperforms the Compensation factor algorithm by 2.56% and 11.5% on DIARETDB1 and DRIVE images respectively. However it is important to notice that, the MRF image reconstruction algorithm depends on the vessel segmentation algorithm, for example if the vessel segmentation algorithm achieved a low performance on severely damage retinal image, the reconstruction would not define a meaningful optic disc region, hence the segmentation will fail.

Further more, the proposed method addresses one of the main issues in medical image analysis, "the overlapping tissue segmentation". Since the blood vessels converse into the optic disc area and misguide the graph cut algorithm through a short path, breaking the optic disc boundary. To achieve a good segmentation results, the MRF image reconstruction algorithm eliminates vessels in the optic disc area without any modification of the image structures before segmenting the optic disc. On the other hand the compensation factor incorporates vessels using local intensity characteristic to perform the optic disc segmentation. Thus our method can be applied in other medical image analysis applications to overcome "the overlapping tissue segmentation."

Our future research will be based on the segmentation of retinal diseases (lesions) known as "exudates" using the segmented structures of the retina (blood vessels and optic disc).Thus a background template can be created using these structures. Then this template can be used to perform the detection of suspicious areas (lesions) in the retinal images.

REFERENCES

[1]. K. Fritzsche, A. Can, H. Shen, C. Tsai, J. Turner, H. Tanenbuam, C. Stewart, B. Roysam, J. Suri, and S. Laxminarayan, "Automated model based segmentation, tracing and analysis of retinal vasculature from digital fundus images," State-of-The-Art Angiography, Applications and Plaque Imaging Using MR, CT, Ultrasound and X-rays, pp. 225–298, 2003.

[2]. A Hoover, V. Kouznetsova, and M. Goldbaum, "Locating blood vessels in retinal images by piecewise threshold probing of a matched filter response," IEEE Transactions on Medical Imaging, vol. 19, no. 3, pp. 203–210, 2000.

[3]. M. Mendonca and A. Campilho, "Segmentation of retinal blood vessels by combining the detection of centerlines and morphological reconstruction," IEEE Transactions on Medical Imaging, vol. 25, no. 9,

[4]. 1200–1213, 2006.

[5]. J. Soares, J. Leandro, R. Cesar, H. Jelinek, and M. Cree, "Retinal vessel segmentation using the 2-d gabor wavelet and supervised classification,"

[6]. IEEE Transactions on Medical Imaging, vol. 25, no. 9, pp. 1214–1222, 2006.

[7]. J. Staal, M. D. Abramoff, M. Niemeijer, M. A. Viergever, and B. van Ginneken, "Ridge-based vessel segmentation in color images of the retina," IEEE Transactions on Medical Imaging, vol. 23, no. 4, pp. 501– 509, 2004.

[8]. S. Chaudhuri, S. Chatterjee, N. Katz, M. Nelson, and M. Goldbaum, "Detection of blood vessels in retinal images using two-dimensional matched filters," IEEE Transactions on medical imaging, vol. 8, no. 3,263–269, 1989.

[9]. F. Zana and J.-C. Klein, "Segmentation of vessel-like patterns using mathematical morphology and curvature evaluation," Image Processing, IEEE Transactions on, vol. 10, no. 7, pp. 1010–1019, 2001.

[10]. L. Xu and S. Luo, "A novel method for blood vessel detection from retinal images," Biomedical engineering online, vol. 9, no. 1, p. 14, 2010.

[11]. M. E. Martinez-Perez, A. D. Hughes, S. A. Thom, A. A. Bharath, and K. H. Parker, "Segmentation of blood vessels from red-free and fluorescein retinal images," Medical image analysis, vol. 11, no. 1, pp. 47–61, 2007.

[12]. L. Zhou, M. S. Rzeszotarski, L. J. Singerman, and J. M. Chokreff, "The detection and quantification of retinopathy using digital angiograms,"

[13]. Medical Imaging, IEEE Transactions on, vol. 13, no. 4, pp. 619–626, 1994.

[14]. Sinthanayothin, J. F. Boyce, H. L. Cook, and T. H. Williamson, "Automated localisation of the optic disc, fovea, and retinal blood vessels from digital colour fundus images," British Journal of Ophthalmology, vol. 83, no. 8, pp. 902–910, 1999.

[15]. R. Chrastek, M. Wolf, K. Donath, H. Niemann, D. Paulus, T. Hothorn, B. Lausen, R. Lammer, C. Y. Mardin, and G. Michelson, "Automated segmentation of the optic nerve head for diagnosis of glaucoma," Medical Image Analysis, vol. 9, no. 1, pp. 297–314, 2005.

[16]. J. Lowell, A. Hunter, D. Steel, A. Basu, R. Ryder, E. Fletcher, and L. Kennedy, "Optic nerve head segmentation," IEEE Transactions on Medical Imaging, vol. 23, no. 2, pp. 256–264, 2004.

[17]. Welfer, J. Scharcanski, C. Kitamura, M. D. Pizzol, L. Ludwig, and D. Marinho, "Segmentation of the optic disc in color eye fundus images using an adaptive morphological approach," Computers in Biology and Medicine, vol. 40, no. 1, pp. 124–137, 2010.

[18]. A Aquino, M. E. Gegundez´-Arias, and D. Mar´ın, "Detecting the optic disc boundary in digital fundus images using morphological, edge detection, and feature extraction techniques," Medical Imaging, IEEE Transactions on, vol. 29, no. 11, pp. 1860–1869, 2010.

[19]. Salazar-Gonzalez, Y. Li, and X. Liu, "Optic disc segmentation by incorporating blood vessel compensation," In Proceedings of IEEE SSCI, International Workshop on Computational Intelligence In Medical Imaging, pp. 1–8, 2011.

[20]. G. Salazar-Gonzalez, Y. Li, and X. Liu, "Retinal blood vessel segmentation via graph cut," in Control Automation Robotics & Vision (ICARCV), 2010 11th International Conference on. IEEE, 2010, 225–230.

[21]. Salazar-Gonzalez, Y. Li, and D. Kaba, "Mrf reconstruction of retinal images for the optic disc segmentation," in Health Information Science. Springer, 2012, pp. 88–99.

[22]. G. S. Gonzalez, "Structure analysis and lesion detection from retinal fundus images," Ph.D. dissertation, Brunel University, 2011.

[23]. Wu, M. Zhang, and J. Liu, "On the adaptive detection of blood vessels in retinal images," IEEE Transactions on Biomedical Engineering, vol. 53, no. 2, pp. 341–343, 2006.

[24]. Y. Y. Boykov and M.-P. Jolly, "Interactive graph cuts for optimal boundary & region segmentation of objects in nd images," in Com-puter Vision, 2001. ICCV 2001. Proceedings. Eighth IEEE International Conference on, vol. 1. IEEE, 2001, pp. 105–112.

[25]. S. Vicente, V. Kolmogorov, and C. Rother, "Graph cut based image seg-mentation with connectivity priors," In Proceedings of IEEE Conference on Computer Vision and Pattern Recognition, CVPR, vol. 1, pp. 1–8, 2008.

[26]. V. Kolmogorov and Y. Boykov, "What metrics can be approximated by geo-cuts, or global optimization of length/area and flux," In Proceedings of Tenth IEEE International Conference on Computer Vision, ICCV., vol. 1, pp. 564–571, 2005.